ISSN 0036-0244, Russian Journal of Physical Chemistry A, 2018, Vol. 92, No. 13, pp. 2618–2627. © Pleiades Publishing, Ltd., 2018.

CHEMICAL KINETICS AND CATALYSIS

A Series of Novel Dendritic Salicylaldimine Iron Catalysts: Synthesis, Characterization, and Application in Ethylene Oligomerization[1]

Jun Wang[a], Yiteng Shang[a], Na Zhang[a], Cuiqin Li[a], and Weiguang Shi[a,*]

[a] *Provincial Key Laboratory of Oil and Gas Chemical Technology, College of Chemistry and Chemical Engineering, Northeast Petroleum University, Daqing, Heilongjiang Province, 163318 China*

**e-mail: sswwgg2003@126.com*

Received October 5, 2017

Abstract—A series of novel dendritic salicylaldimine ligands and their corresponding iron complexes have been synthesized using 1.0 generation (1.0 G) dendritic macromolecules, salicylaldehyde and $FeCl_2 \cdot 4H_2O$ as raw materials. The structures of the ligands and iron complexes were characterized by FT-IR, ^1H NMR, UV, ESI-MS, and elemental analysis. The dendritic salicylaldimine iron complexes presented moderate catalytic activity in ethylene oligomerization and selectivity for higher carbon number olefins products ($\geq C_8$) when they were activated with methylaluminoxane (MAO). The catalytic activity and product selectivity were related to the co-catalyst, solvent, bridged group length and reaction parameters such as reaction temperature, Al/Fe molar ratio and ethylene pressure. The complex C3 showed the highest catalytic activity (up to 13.75×10^4 g (mol Fe h)$^{-1}$) and the selectivity of higher carbon number olefins (35.31%) at the optimized conditions. Moreover, the catalytic properties of dendritic salicylaldimine iron complex C3 was better than non-dendritic iron complex.

Keywords: dendritic macromolecule, iron complex, ethylene oligomerization, catalytic activity, selectivity

DOI: 10.1134/S0036024418130162

INTRODUCTION

Ethylene oligomerization is currently one of the major industrial processes for producing linear α-olefins, which are main industrial substance widely used for preparation of detergents, lubricants field chemicals, and as co-monomers for copolymerization [1–3]. Since Ziegler's original work on AlR_3 catalysis of ethylene oligomerization [4], developing new oligomerization catalysts with various transition metals such as nickel, chromium, titanium, zirconium, and others have been considerable sustained interest in both academic and industrial fields [5–11]. A great number of published works concerning the oligomerization reaction were devoted to nickel complexes [12–18]. However, in recent years, the iron and cobalt complexes based on different structures are known as highly active catalysts for the oligomerization of ethylene, and such systems are currently the focus of much research [19–21]. Compared with other transition metals, iron is the most abundant transition metal on the earth with the content of 5.1% after oxygen, silicon and aluminium, and is one of the most inexpensive and environmentally friendly metals. Moreover, iron complexes could be as catalytic active site for ethylene oligomerization with high catalytic activity and selectivity for linear α-olefins [22–25].

Schiff base ligands have been synthesized and used in number of catalytic reactions [26]. In particular the salicylaldimine ligands can coordinate with metals through hard nitrogen and oxygen donor atoms, which lead to better stabilization of metal complexes against reduction and confers unusual thermal stability [27]. Therefore the metal complexes with the Schiff base ligands have been used extensively in ethylene oligomerization. We have reported the preparation of the dendritic nickel and cobalt complexes containing Schiff base ligands, and the research results showed that the dendritic nickel and cobalt complexes exhibited excellent catalytic properties for ethylene oligomerization [28, 29]. In this paper, we synthesized a series of dendritic salicylaldimine iron complexes with 1.0 G dendritic macromolecules, salicylaldehyde and ferrous chloride tetrahydrate as raw materials. We looked into the possibility of these complexes as catalysts being able to produce higher carbon number olefins and also investigated the effects of solvent, co-catalyst, and reaction conditions on ethylene oligomerization,

[1] The article is published in the original.

along with the effect of the structure of catalysts on ethylene oligomerization.

EXPERIMENTAL

Materials and General Considerations

All experimental works of air and moisture sensitive compounds were performed under a nitrogen atmosphere using standard Schlenk techniques. All the solvents were analytical grade and dried by refluxing over sodium/benzophenone and distilled under nitrogen prior to use. MAO (10 wt % in toluene) and ethylaluminum sesquichloride (EASC, 25 wt % in cyclohexane) were offered by Sigma-Aldrich (China). Toluene and methanol were purchased from Tianjin Kermel Chemical Reagent Co., Ltd. (China). *n*-Hexane was obtained from Tianjing Damao Chemical reagent factory. Salicylaldehyde was provided by Tianjin Guangfu Fine Chemical Research Institute (China). 1.0 G dendritic macromolecules with 1,2-ethylenediamine, 1,4-butanediamine, and 1,6-hexanediamine as cores were synthesized according to [30]. $FeCl_2 \cdot 4H_2O$ were purchased from Tianjin Damao Chemical Reagent Factory (China).

IR spectra were recorded in a KBr disc matrix using a Bruker Vector 22 IR spectrophotometer over the range of 4000–450 cm^{-1}. ^1H-NMR spectrum was recorded with Bruker-400 MHz NMR at 400 MHz in $CDCl_3$ with tetramethylsilane (TMS) as an internal reference. The UV–Vis spectra were carried out on a UV-1700 ultraviolet-visible spectrophotometer with methanol as solvent. Elemental analyses were carried on the Optima 5300DV analyzer (America). Electrospray ionization mass spectrometry (ESI-MS) data were collected on an micrOTOF-Q II mass spectrometer. GC-MS analyses were performed on Agilent equipped with a flame ionization detector (FID) and a 30 m (0.25 mm i.d., 0.25 μm film thickness) DB-1 column. Gas chromatography (GC) analyses of oligomers were performed on a Fuli GC9720 equipped with a flame ionization detector (FID) and a 50 m (0.2 mm i.d., 0.5 μm film thickness) HP-PONA column.

Synthesis of Dendritic Salicylaldimine Ligands

Methanol (30 mL) was added to the mixture of 1.0 G dendritic macromolecule S1 (1.55 g, 3 mmol) and $NaSO_4$ (3 g) under the nitrogen atmosphere, and the solution of the mixture was stirred for 10 min at 25°C. Then salicylaldehyde (2.60 mL, 24 mmol) was added dropwise after the solution being heated to 65°C and was refluxed for 12 h. The dendritic salicylaldimine ligand solution was obtained after removing $NaSO_4$ by filtration. The ligand solution crystallized for 48 h at –30°C. A yellow precipitate was formed and was isolated by filtration, washed three times with ether and dried in vacuum, affording dendritic salicylaldimine ligand L1 as a yellow solid. Yield: 1.60 g (57%); IR (KBr, cm^{-1}): 3436 (s), 2946 (w), 1644 (s), 1459 (m), 752 (m); ^1H NMR (400 MHz, $CDCl_3$, ppm): δ: 8.354 (N=CH), 8.273 (nh), 7.285 (CH, benzene), 7.233 (CH, benzene), 6.946 (CH, benzene), 6.853 (CH, benzene), 5.299 (OH), 3.932 ($C\underline{H_2}N{=}CH$), 3.685 (CH_2, $C\underline{H_2}NH$), 3.521 (CH_2N), 3.089 (CH_2, bridged group), 2.296 (CH_2CO); λ_{max} (nm): 214, 254, 323.

Dendritic salicylaldimine ligands L2 and L3 were synthesized through the reaction between 1.0 G dendritic macromolecules (S2 and S3) and salicylaldehyde according to the method described in the literatures [28, 29].

Synthesis of Dendritic Salicylaldimine Iron Complexes

A methanol solution (15 mL) of dendritic salicylaldimine ligand L1 (4.65 g, 0.005 mol) was added to a methanol solution (5 mL) of $FeCl_2 \cdot 4H_2O$ (3.98 g, 0.02 mol). The reaction mixture turned into dark red immediatedly and was allowed to stir at 25°C for 24 h. The precipitate was obtained after diethyl ether being added to the mixture. The resultant precipitate was then isolated by filtration, and washed with diethyl ether to afford complex C1 as a red solid. Yield: 4.06 g (78%) (Scheme 1); IR (KBr, cm^{-1}): 3398 (s), 2928 (w), 1611 (s), 1546 (m), 764 (m); anal. calcd. for $C_{50}H_{60}N_{10}O_8Fe_2$: Fe, 10.76; found: Fe, 9.97; λ_{max} (nm): 233, 256, 323; ESI-MS: *m/z*: 1042 $[M+H]^+$, 929 $[M-2Fe]^+$.

Complex C2 was prepared according to the procedure used for the synthesis of complex C1 using ligand L2 (4.79 g, 0.005 mol) and $FeCl_2 \cdot 4H_2O$ (3.98 g, 0.02 mol). Yield: 4.28 g (80%) (Scheme 1); IR (KBr, cm^{-1}): 3398 (s), 2929 (w), 1607 (s), 1535 (m), 753 (m); anal. calcd. for $C_{52}H_{64}N_{10}O_8Fe_2$: Fe, 10.49; found: Fe, 9.85; λ_{max} (nm): 234, 261 321; ESI-MS: *m/z*: 1069 $[M+H]^+$, 957 $[M-2Fe]^+$.

Complex C3 was prepared according to the procedure used for the synthesis of complex C1 using ligand L3 (4.92 g, 0.005 mol) and $FeCl_2 \cdot 4H_2O$ (3.98 g, 0.02 mol). Yield: 4.16 g (76%) (Scheme 1); IR (KBr, cm^{-1}): 3397 (s), 2953 (w), 1611 (s), 1541 (m), 764 (m); anal. calcd. for $C_{54}H_{68}N_{10}O_8Fe_2$: Fe, 10.22; found: Fe, 9.64; λ_{max} (nm): 236, 260, 323; ESI-MS: *m/z*: 1096 $[M+H]^+$, 984 $[M-2Fe]^+$.

General Process for Ethylene Oligomerization

All ethylene oligomerization tests were performed in a 250 mL stainless steel reactor with magnetic stirring, temperature controller and an internal cooling system. The reactor was dried in an oven at 160°C for 3 h prior to each run, and then cooled to the required temperature. After evacuation and flushing with ethylene three times, a typical reaction was performed by introducing solvent (40 mL), the proper amount of

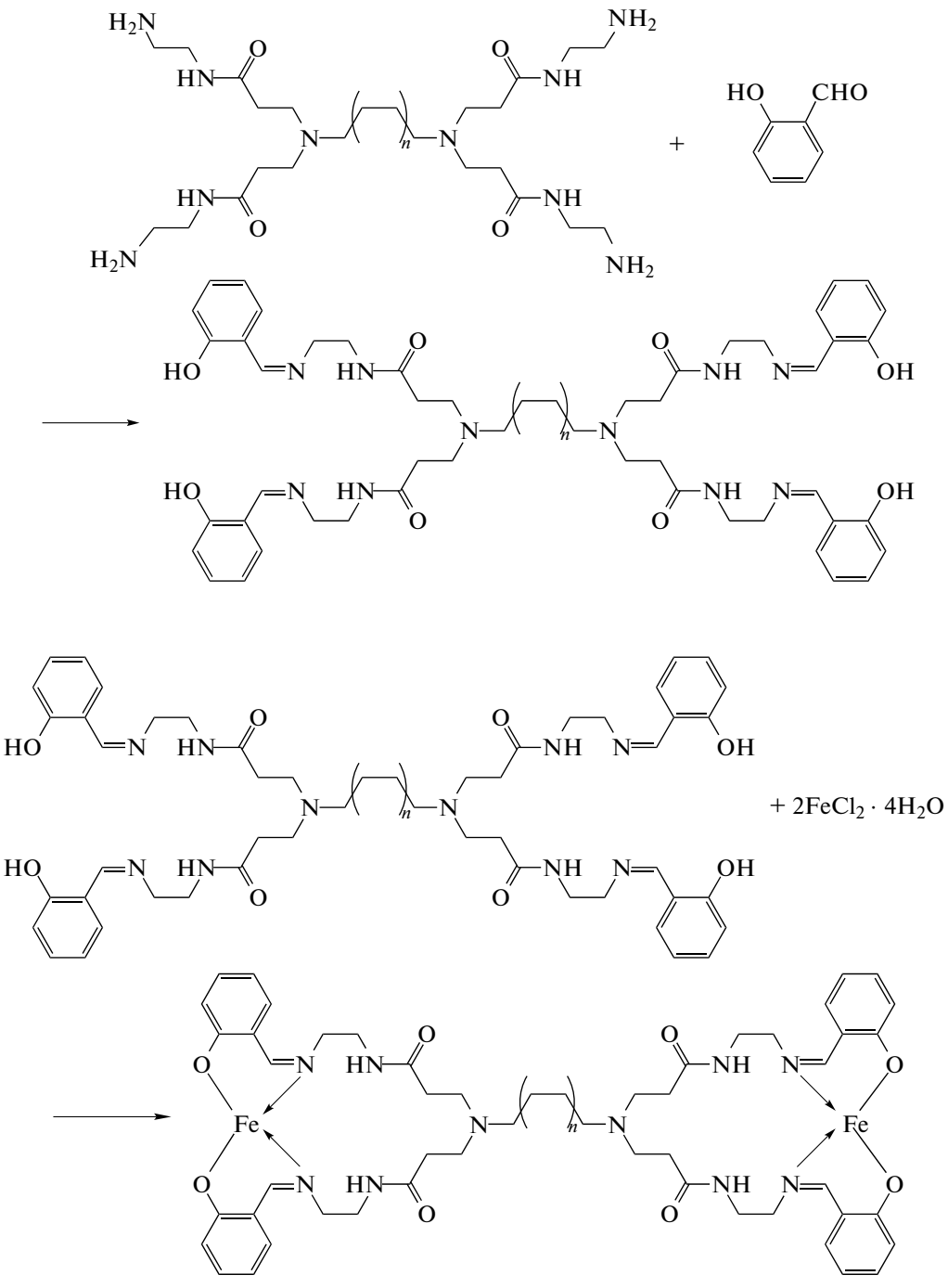

Scheme 1. Synthetic routes of dendritic salicylaldimine iron complexes.

co-catalyst (MAO or EASC) and the catalyst solution (10 mL, [Fe] = 5 μmol) were injected into the reactor under a stream of ethylene and then the reactor was immediately pressurized. Ethylene was continuously fed in order to maintain the ethylene pressure. After the desired time, the reaction was quenched by cooling the system to 0°C, depressurizing and adding HCl/ethanol (10 wt %). The catalytic activity was calculated based on the increase of product weight. The mixture was analyzed by GC or GC-MS to gain the

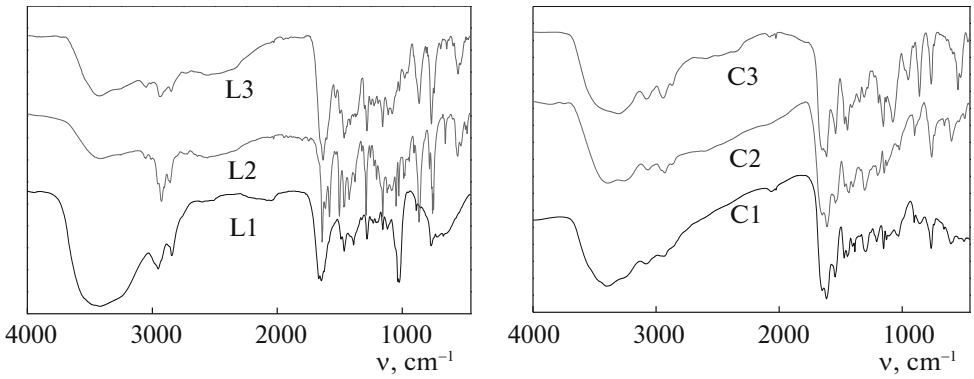

Fig. 1. FT-IR spectra of the dendritic salicylaldimine ligands and iron complexes.

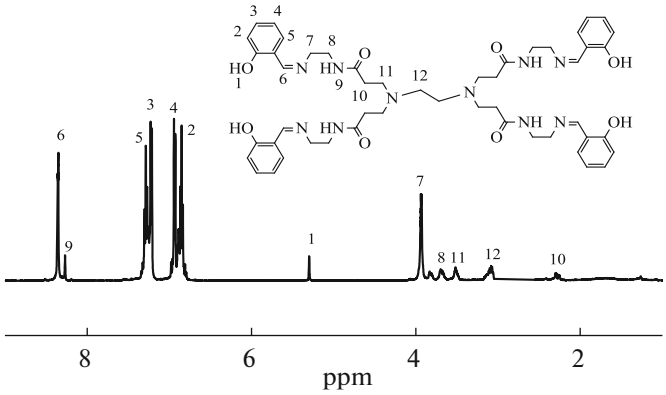

Fig. 2. ^{1}H NMR spectrum of the dendritic salicylaldimine ligand L1.

selectivity of catalysts by comparison to the standard authentic samples.

RESULTS AND DISCUSSION

Characterization of Dendritic Salicylaldimine Ligands and Iron Complexes

FT-IR Spectroscopy. The FT-IR spectra of the dendritic salicylaldimine ligands L1-L3 and the iron complexes C1-C3 are shown in Fig. 1. As can be seen from the spectra of the dendritic salicylaldimine ligands, the characteristic peaks at around 2946 cm^{-1} were designated to the stretching vibration of $-CH_2-$ groups. The peaks at approximately 1459 cm^{-1} belonged to the stretching vibration of benzene ring. The absorption peaks at around 3436 cm^{-1} were due to the overlap of stretching vibration of –NH– and –OH groups. The peaks at around 1644 cm^{-1} belonged to the stretching vibration of the C=N groups, which indicated that the Schiff base reactions were proceed between 1.0 G dendritic macromolecules and salicyladehyde. Compared with the spectra of the dendritic salicylaldimine ligands, the absorption peaks of C=N stretching vibration were shifted to a lower wave number at around 1611 cm^{-1}, which indicated that the metal ions had coordinated with the imino nitrogen atoms and the oxygen atoms of the ligands.

^{1}H NMR Spectroscopy. ^{1}H NMR spectrum of the dendritic salicylaldimine ligand L1 is shown in Fig. 2. The signal for the protons in the methylene groups which belonged to the bridged group could be found at around 3.089 ppm. The signal for the protons in α-methylene connected to tertiary amine group was evidenced at around 3.521 ppm. The signal for the protons in methylene connected to carbonyl group was exhibited at around 2.296 ppm. The signal for the protons in methylene group connected to secondary amine group was evidenced by the peak at around 3.658 ppm. The signal for the protons in the secondary amine group was indicated at around 8.273 ppm. The signal for the protons in the methylene connected to imine and benzene occurred at around 8.354 ppm. The signal for the protons in aryl rings occurred at around 6.853–7.285 ppm. In addition, the signal for the protons in hydroxyl connected to benzene occurred at around 5.299 ppm. Above signal for the protons further indicated that the Schiff base reaction occurred between 1.0G dendritic macromolecule S1 and salicyladehyde.

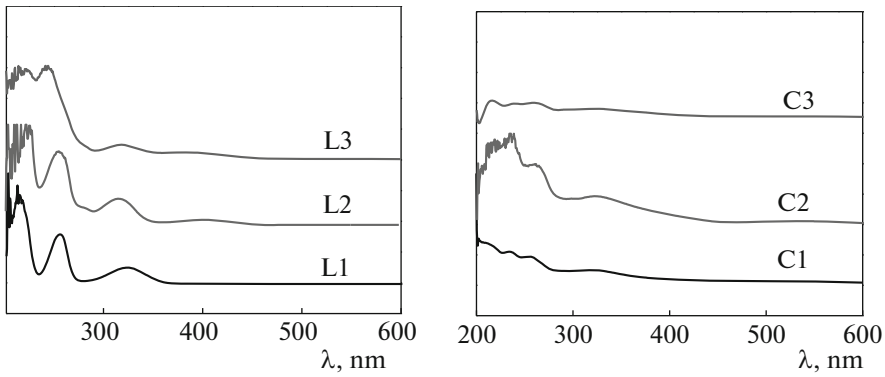

Fig. 3. UV spectra of the dendritic salicylaldimine ligands and iron complexes.

UV spectroscopy. The UV spectra of the dendritic salicylaldimine ligands and iron complexes are given in Fig. 3. The UV spectra of the dendritic salicylaldimine ligands in the methanol solution showed three absorption bands at around 214, 254, and 323 nm. The bands at around 214 nm should be ascribed to the R band of $n \rightarrow \pi^*$ transition for C=O, the bands at around 254 nm were assigned to the B band of the benzene ring, and the bands at around 323 nm belonged to the R band of $n \rightarrow \pi^*$ transition for C=N. The UV spectra of iron complexes showed that the R band of the C=O and the B band of the benzene ring occurred slightly shift to around 234 and 260 nm, respectively. Meanwhile, the visibly weak peaks of $n \rightarrow \pi^*$ transition for C=N at around 323 nm were observed, indicating that the iron atom was involved in coordination to the dendritic salicylaldimine ligands.

MS spectroscopy. The MS spectra of the dendritic salicylaldimine iron complexes are given in Fig. 4. As shown in Fig. 4, the molecular ion peaks of the dendritic salicylaldimine iron complexes C1, C2, and C3 appeared at *m/z*: 1042, 1069, and 1096, respectively. The loss of 2Fe resulted in the formation of the base peaks at *m/z*: 929, 957, and 984, corresponding to the dendritic salicylaldimine ligands. Above data indicated that the actual values were accordant with the theoretical values.

Ethylene oligomerization. Dendritic salicylaldimine iron complexes C1–C3 were evaluated as catalysts for oligomerization of ethylene, using two co-catalysts (MAO and EASC) and three solvents (toluene, chlorobenzene and *n*-hexane) in attempt to generate active catalysts. The research results showed that all the complexes produced active catalysts for the oligomerization of ethylene and the reaction conditions, solvent, co-catalyst, bridged group length as well as catalyst structure had a significant effect on catalytic activity and oligomer distribution.

Effect of co-catalyst on the catalytic activity and oligomer distribution. The dendritic salicylaldimine iron complexes C1, C2, and C3 were activated with MAO and EASC in toluene solvent so as to research the effect of the co-catalysts on catalytic activity and oligomer distribution at the same ethylene oligomerization reaction conditions and the research results are listed in Table 1. As showed in Table 1, the co-catalyst had a crucial effect on catalytic activity. Upon activation with MAO, the iron complexes C1, C2, and C3 showed lower catalytic activities (activity varying from 5.59×10^4 to 6.79×10^4 g(mol Fe h)$^{-1}$). However, activation the iron complexes C1, C2 and C3 with co-catalyst EASC instead of co-catalyst MAO, the catalytic activities were higher than the catalytic system with MAO as co-catalyst (activity varying from 24.35×10^4 to 39.37×10^4 g (mol Fe h)$^{-1}$). As for higher activity with co-catalyst EASC that possible reason due to the electron shielding effect can be decreased and the strong Lewis acid can increase the metal active sites to generate the high catalytic activity. In addition, the co-catalyst also had a significant effect on oligomer distribution. When activated the iron complexes C1, C2, and C3 with MAO, the oligomerized ethylene to afford C_4 as the major product and C_6 and higher carbon number olefins. The observed selectivity with MAO as co-catalyst would be consistent with a faster

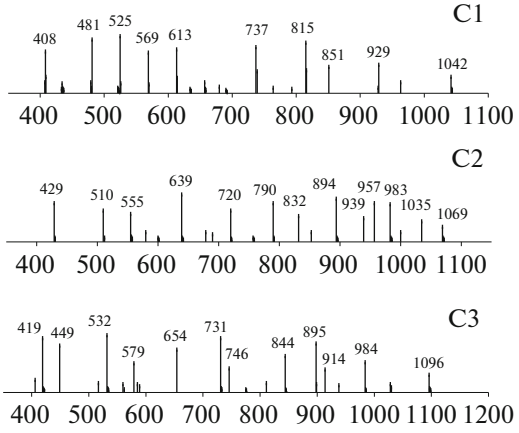

Fig. 4. MS spectra of the dendritic salicylaldimine iron complexes.

Table 1. Effect of co-catalyst on the catalytic activity and oligomer distribution[a]

Entry	Complexes	Co-catalytic	Activity 10^4 g (mol Fe h)$^{-1}$	Oligomer distribution, %				
				C_4	C_6	$\leq C_6$[d]	C_8	C_8–C_{18}[e]
1[b]	C3	MAO	6.79	52.7	9.9	62.6	18.3	37.4
2[c]	C3	EASC	39.37	12.8	19.8	32.6	5.3	67.4
3[b]	C2	MAO	6.12	60.8	21.5	82.3	8.6	17.7
4[c]	C2	EASC	33.19	8.6	14.7	23.3	7.1	76.7
5[b]	C1	MAO	5.59	78.4	12.6	91.0	6.3	9.0
6[c]	C1	EASC	24.35	11.7	13.6	25.3	5.9	74.7

[a] Reaction condition: [Fe] = 5 μmol, [toluene] = 50 mL, time = 30 min, temperature = 15°C, Al/Fe = 300, pressure = 0.5 MPa.
[b] 10^4 g (mol Fe h)$^{-1}$.
[c] Determined by GC.
[d] Low carton number olefins.
[e] Higher carton number olefins.

Table 2. Effect of solvent on the catalytic activity and oligomer distribution[a]

Entry	Complexes	Solvent	Activity 10^4 g (mol Fe h)$^{-1}$	Oligomer distribution, %[b]				
				C_4	C_6	$\leq C_6$[c]	C_8	C_8–C_{18}[d]
1	C3	Toluene	6.79	52.7	9.9	62.6	18.3	37.4
2	C3	*n*-Hexane	1.29	66.8	23.0	89.8	9.8	10.2
3	C3	Chlorobenzene	20.57	83.7	7.2	90.9	3.5	9.1
4	C2	Toluene	6.12	60.8	21.5	82.3	8.6	17.7
5	C2	*n*-Hexane	1.02	69.4	20.6	90.0	6.7	10.0
6	C2	Chlorobenzene	13.59	85.8	9.5	95.3	4.0	4.7
7	C1	Toluene	5.59	78.4	12.6	91.0	6.3	9.0
8	C1	*n*-Hexane	1.01	74.2	18.9	93.1	5.2	6.9
9	C1	Chlorobenzene	10.67	87.6	10.2	97.8	2.1	2.2

[a] Reaction condition: [Fe] = 5 μmol, [solvent] = 50 mL, time = 30 min, Al/Fe = 300, temperature = 15°C, ethylene pressure = 0.5 MPa.
[b] Determined by GC.
[c] Lower carton number olefins.
[d] Higher carton number olefins.

rate of β-hydrogen elimination relative to that of chain growth. When activated the iron complexes C1, C2, and C3 with EASC in toluene solvent produced a small amount of oligomers C_4, C_6, and C_8, as well as predominantly alkylated-toluenes of the pre-formed oligomers (C_4 and C_6 as minor products). The above experiment results showed that although the catalytic activities were higher when EASC was used as co-catalyst, the products were mainly alkylated–toluenes of the pre-formed oligomers. Comprehensive consideration, co-catalyst MAO was selected for all further investigations.

Effect of solvent on the catalytic activity and oligomer distribution. The solvent can influence the catalytic activity and product distribution due to the solubility of the catalyst itself. Considering the kind of solvent in ethylene oligomerization reactions, complexes C1, C2, and C3 were further investigated in *n*-hexane and chlorobenzene, which were compared with the previous results in toluene and the results are listed in Table 2. The catalytic activities decreased under similar conditions in the order of *n*-hexane < toluene < chlorobenzene. Because complexes C1, C2, and C3 have poor solubility in *n*-hexane the, so catalytic activities were the lowest than those in toluene and chlorobenzene. This was because chlorobenzene and toluene has bigger polarity than *n*-hexane, and they favour having good solubility of the complexes in ethylene oligomerization reaction. In addition, it is interesting to note that the selectivity of higher carbon number olefin was higher with toluene as solvent than *n*-hexane and chlorobenzene. Therefore, further catalytic studies were performed with toluene as solvent.

Table 3. Influence of reaction conditions on the catalytic activity and oligomer distribution[a]

Entry	Al/Fe	T, °C	P, MPa	Activity 10^4 g(mol Fe h)$^{-1}$	Oligomer distribution, %[b]				
					C_4	C_6	$\leq C_6$[c]	C_8	C_8–C_{18}[d]
1	300	15	0.5	6.79	52.7	9.9	62.6	18.3	37.4
2	300	25	0.5	6.47	51.9	21.8	73.7	7.6	26.3
3	300	35	0.5	5.61	47.8	25.1	72.9	7.9	27.1
4	300	45	0.5	5.31	45.9	23.1	69.0	11.1	31.0
5	300	15	0.5	6.79	52.7	9.8	62.5	18.3	37.5
6	500	15	0.5	8.34	59.0	14.7	73.7	10.2	26.3
7	700	15	0.5	8.76	61.0	21.4	82.4	9.2	17.6
8	1000	15	0.5	13.82	66.5	19.2	85.7	7.1	14.3
9	500	15	0.1	6.34	65.5	19.4	84.9	8.7	15.1
10	500	15	0.5	8.34	59.0	14.7	73.7	10.2	26.3
11	500	15	0.7	11.98	53.6	16.2	69.8	12.1	30.2
12	500	15	1.0	13.75	49.3	15.4	64.7	18.3	35.3

[a] Reaction condition: [Fe] = 5 μmol, [toluene] = 50 mL, time = 30 min, MAO as co-catalyst.
[b] Determined by GC.
[c] Lower carton number olefins.
[d] Higher carton number olefins.

The length of bridged group had a significant influence on the catalytic activities and oligomer distribution, which can be seen from Tables 1 and 2. It was apparent that the catalytic active increased with the increase of bridged group length. The complex C3 with the longest bridged group length displayed the highest catalytic activity compared to the complexes C1 and C2 (Tables 1 and 2). This could be explained that the solubility of the complex increased with the increase of the bridged group length, which led to the increase of the concentration of the effective active species in the catalyst system. Not only the catalytic activity was sensitive to the length of bridged group, but also the selectivity of higher carbon number olefins was significantly affected by the length of bridged group. The concentration of higher carbon number olefins increased with the increase of the bridged group length.

Influence of reaction conditions on the catalytic activity and oligomer distribution. It is well known that the reaction conditions have significant effect on catalytic activity and oligomer distribution. The complex C3 was investigated under varying conditions, such as reaction temperature, ethylene pressure and the amount of MAO in order to probe the effects of reaction parameters on the catalytic activity and oligomer distribution. The oligomerization results are summarized in Table 3. As revealed in Table 3, the reaction temperature significantly affected the catalytic activity and oligomer distribution. Increasing the reaction temperature from 15 to 45°C led to decrease of the catalytic activity (Table 3, entries 1–4). With increased temperature, which might be attributable to decomposition of the active species and it will quicken deactivated ratio of catalyst [31, 32]. Meanwhile, ethylene solubility decreased at higher temperature. All the results indicated that although enhanced reaction temperature were excepted to result in overall higher propagation and transfer rates, chain propagation rate and chain transfer rate did not present linear relationship, which could result in that the oligomer distribution did not present obvious change rule with the increase of reaction temperature.

The effect of the Al/Fe molar ratio on the catalytic activity and oligomer distribution were further investigated with complex C3. The catalytic activities increased with increasing of the Al/Fe molar ratio in the range 300 to 1000 (Table 3, entries 5–8), and the highest activity of 13.82×10^4 g/(mol Fe h) was observed at an Al/Fe molar ratio of 1000 at 15°C. Higher Al/Fe molar ratio resulted in increased catalytic activity, which possibly due to that MAO scavenged adventitious water and impurities in the solvent at low Al/Fe molar ratio and the iron complex required more co-catalyst to be activated to produce more active species, which make more ethylene monomer react with active species. Generally higher Al/Fe molar ratio decreases the formation of higher carbon number olefins (Table 2, entries 5–8). This trend would be attributed to increased chain transfer to the co-catalyst or greater chain termination due to increased catalytic activities.

The influence of ethylene pressure on the catalytic activity and oligomer distribution was studied by varying ethylene pressure from 0.1 to 1.0 MPa with complex C3 (Table 3, entries 9–12). From the results, an

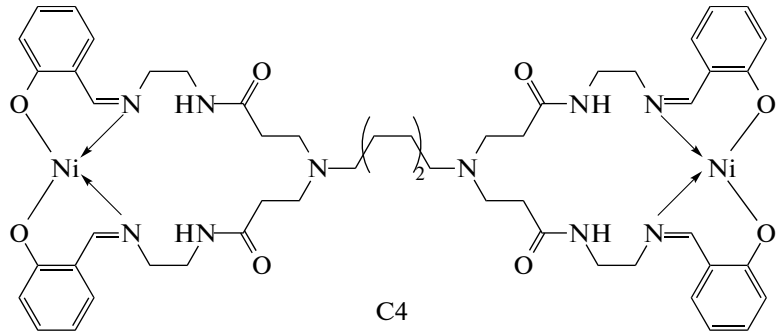

C4

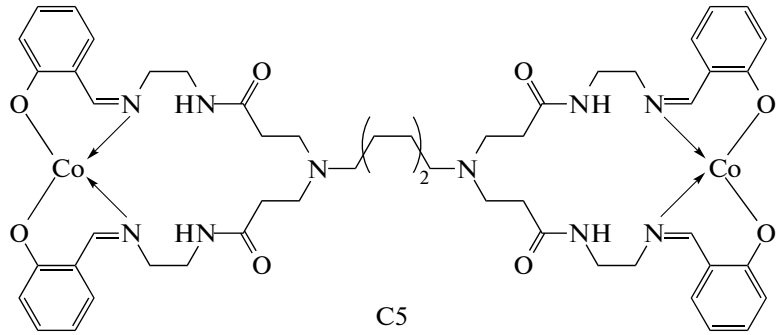

C5

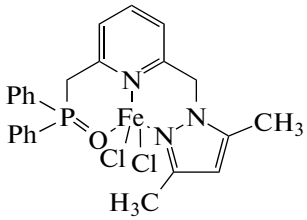

C6

Fig. 5. The structures of dendritic nickel, cobalt complexes and (pyrazolyl)-(phosphinoyl) pyridine iron complex.

increase in ethylene pressure from 0.1 to 1.0 MPa led to increased catalytic activities from 6.34×10^4 to 13.75×10^4 g/(mol Fe h). The reason was that the ethylene solubility dependence on pressure. In addition, we also found that a change of ethylene pressure had an effect on the product distribution. With increasing of ethylene pressure, the formation of the higher carbon number olefins was easier. Higher composition of higher carbon number olefins at higher pressures suggested that increasing ethylene pressure had a heavier impact on the chain propagation than on the β-H elimination in the oligomerization process.

Influence of catalyst structure on the catalytic activity and oligomer distribution. The influence of catalyst structure on the catalytic activity and oligomer distribution was studied using the dendritic iron complex C3, dendritic nickel complex C4 (Fig. 5), dendritic cobalt complex C5 (Fig. 5), and (pyrazolyl)-(phosphinoyl) pyridine iron complex C6 (Fig. 5) which was synthesized by Nyamato et al. [33] and the results are summarized in Table 4. The metal atom had a significant effect on the catalytic activity. The dendritic nickel complex C4 displayed higher catalytic activity compared to dendritic cobalt complex C5 and dendritic iron complex C3. One plausible reason for this trend could be attributable to that the electron density of nickel atom is larger than cobalt atom and iron atom, and the nickel active center was easy to form and had better stability than cobalt center and iron center under the MAO activation. In addition, as can be seen from table 4, the ligand type also had a considerable impact on the catalytic activity. It was apparent that the catalytic activity of dendritic iron complex C3 was higher than (pyrazolyl)-(phosphinoyl) pyridine iron complex C6. The finding was due to that the dendritic iron complex C3 had double the amount of iron active centers than the (pyrazolyl)-(phosphinoyl) pyridine iron complex C6. There were much more ethylene molecules reaction with iron active centers in unit time when the dendritic iron complex C3 was used.

We also observed the dependence of oligomer distribution on catalyst structure. The dendritic nickel

Table 4. Effect of catalyst structure on the catalytic activity and oligomer distribution[a]

Entry	Complexes	Activity 10^5 g(mol Fe h)$^{-1}$	Oligomer distribution, %[b]				
			C_4	C_6	$\leq C_6$[c]	C_8	C_8–C_{18}[d]
1	C3	1.22	59.4	20.2	79.6	9.7	20.4
2	C4	2.37	45.9	17.2	63.1	35.3	36.9
3	C5	1.89	32.5	11.6	44.1	20.4	55.9
4	C6	1.10	94.0	6.0	100.0	–	–

[a] Reaction condition: [Fe] = 10 μmol, [toluene] = 80 mL, time = 30 min, temperature = 30°C, Al/M = 250, pressure = 1.0 MPa.
[b] Determined by GC.
[c] Lower carton number olefins.
[d] Higher carton number olefins.

and cobalt complexes preferred to higher carbon number olefins compared with the dendritic iron complex. For example, the dendritic iron complex gave the selectivity of 20.47% for higher carbon number olefins, and the dendritic nickel and cobalt complex gave the selectivity of 36.95% and 55.83% for higher carbon number olefins, respectively. However, the selectivity of higher carbon number olefins of the dendritic iron complex was higher than the (pyrazolyl)-(phosphinoyl) pyridine iron complex, which indicated that the dendritic metal catalysts had good application prospect in the field of ethylene oligomerization.

CONCLUSION

Three novel dendritic salicylaldimine iron catalysts have been synthesized, structurally characterized and used for ethylene oligomerization. Activation of these catalysts with MAO and EASC to afford lower carbon number olefins and alkylated toluenes as the major products, respectively. Both the catalytic activity and oligomer distribution were largely dependent on the nature of the co-catalyst, nature of the solvent, reaction conditions and the length of bridged group. The dendritic salicylaldimine iron catalysts exhibited moderate catalytic activity and selectivity of higher carbon number olefins. While the processes of synthetic for dendritic salicylaldimine iron catalyst was complicated, its superiority lied in its higher catalytic activity and selectivity of higher carbon number olefins compared with the iron catalyst bearing the non-dendritic ligand. However, the catalytic activity and the selectivity of higher carbon number olefins of dendritic iron catalyst were less than dendritic nickel and cobalt catalysts. A key component of catalyst design thus further demonstrating that the dendritic metal catalysts have better catalytic activity and selectivity of higher carbon number olefins than the non-dendritic metal catalysts, especially dendritic nickel catalyst.

ACKNOWLEDGMENTS

We acknowledge the funding from the Natural Science Foundation of China (no. 21576048), Petroleum Innovation Foundation of China (no. 2014D-5006-0503) and Youth Science Foundation of Northeast Petroleum University (2013NQ130).

REFERENCES

1. A. Finiels, F. Fajula, and V. Hulea, Catal. Sci. Technol. **4**, 2412 (2014).
2. J. X. Hou, W. H. Sun, D. H. Zhang, L. Y. Chen, W. Li, D. F. Zhao, and H. B. Song, Appl. Catal. A **231**, 221 (2005).
3. P. A. R. Breuil, L. Magnal, and H. Olivier-Bourbigou, Catal. Lett. **145**, 173 (2015).
4. W. Keim, F. H. Kowaldt, R. Goddard, and C. Kruger, Angew. Chem. Int. Ed. **17**, 466 (1978).
5. A. Asma, D. A. Radu, A. Samira, C. Claudia, N. Djamel, and H. Vasole, Appl. Clay Sci. **146**, 432 (2017).
6. L. Chen, J. Hou, and W. Sun, Appl. Catal., A **246**, 11 (2003).
7. D. J. Martin, B. D. McCarthy, N. A. Piro, and J. L. Dempsey, Polyhedron **114**, 200 (2016).
8. S. Hameury, P. D. Frémont, P. A. R. Breuil, H. Olivier-Bourbigou, and P. Braunstein, Organometallics **34**, 2183 (2015).
9. F. He, W. Z. Zhao, X. P. Cao, T. L. Liang, C. Redshaw, and W. H. Sun, J. Organomet. Chem. **713**, 209 (2012).
10. W. Keim, Angew. Chem. Int. Ed. **52**, 12492 (2013).
11. A. Boudier, P. A. R. Breuil, L. Magna, H. O. Bourbigou, and P. Braunstein, Chem. Commun. **50**, 1398 (2014).
12. A. Boudier, P. R. A. Breuil, L. Magna, H. Olivier-Bourbigou, and P. Braunstein, J. Organomet. Chem. **718**, 31 (2012).
13. A. H. D. P. S. Ulbrich, R. R. Campedelli, J. L. S. Milani, J. H. Z. D. Santos, and O. D. L. Casagrande, Appl. Catal., A **453**, 280 (2013).
14. W. W. Zuo, C. Tourbillon, V. Rosa, K. Cheaib, M. M. Andrade, S. Dagorne, and R. Welter, Inorg. Chim. Acta **383**, 213 (2012).

15. F. Martínez-Olid, E. D. Jesús, and J. C. Flores, Inorg. Chim. Acta **409**, 156 (2014).
16. V. A. Tuskaev, S. C. Gagieva, D. A. Kurmaev, T. M. Zvukova, I. V. Fedyanin, and B. M. Bulychev, Inorg. Chim. Acta **442**, 167 (2016).
17. R. D. Andrei, M. I. Popa, F. Fajula, and V. Hulea, J. Catal. **323**, 76 (2015).
18. S. B. Zou, X. F. Wang, C. C. Du, D. Z. Wang, and D. Z. Jia, CrystEngComm (2017). doi 10.1039/C7CE00394C
19. P. Hao, Y. J. Chen, T. P. F. Xiao, and W. H. Sun, J. Organomet. Chem. **695**, 90 (2010).
20. M. N. Alnajrani and F. S. Mair, Dalton Trans. **45**, 10435 (2016).
21. M. K. Ainooson, I. A. Guzei, L. C. Spencer, and J. Darkwa, Polyhedron **53**, 295 (2013).
22. B. L. Small and M. Brookhart, J. Am. Chem. Soc. **120**, 7143 (1998).
23. B. L. Small, M. Brookhart, and A. M. A. Bennett, J. Am. Chem. Soc. **120**, 4049 (1998).
24. C. Görl, T. Englmann, and H. G. Alt, Appl. Catal., A **403**, 25 (2011).
25. Z. C. Zhang, S. T. Chen, X. F. Zhang, H. Y. Li, Y. C. Ke, Y. Y. Lu, and Y. L. Hu, J. Mol. Catal., A **230**, 1 (2005).
26. V. C. Gibson, C. Redshaw, and G. A. Solan, Chem. Rev. **107**, 1745 (2007).
27. R. Eaves, S. Parkin, and F. T. Ladipo, Inorg. Chem. Acta **46**, 9500 (2007).
28. J. Wang, H. Y. Li, L. Song, W. G. Shi, N. Zhang, and C. Q. Li, J. Macromol. Sci. A **53**, 709 (2016).
29. J. Wang, L. L. Ma, L. Song, S. H. Wang, H. L. Huo, and C. Q. Li, Chem. Pap. **71**, 895 (2016).
30. J. Wang, C. Q. Li, S. Y. Zhang, F. Sun, and T. J. Ge, Chin. Chem. Lett. **19**, 43 (2008).
31. J. X. Li, Z. X. Du, J. Zhou, H. Q. An, S. R. Wang, B. L. Zhu, S. M. Zhang, S. H. Wu, and W. P. Huang, Inorg. Chem. Acta **362**, 4884 (2009).
32. K. F. Wang, K. Wedeking, W. W. Zuo, D. H. Zhang, and W. H. Sun, J. Organomet. Chem. **693**, 1073 (2008).
33. G. S. Nyamato, M. G. Alam, S. O. Ojwach, and M. P. Akerman, J. Organomet. Chem. **783**, 64 (2015).